CIVIL ENGINEERING JOURNAL

Article no. 16

THE CIVIL ENGINEERING JOURNAL 1-2021

DISPLACEMENTS OF SIDE WALLS WITH WALL-GIRTS IN INDUSTRIAL BUILDINGS UNDER VERTICAL SETTLEMENTS

Noemí M. Subelza[1], Verónica A. Pedrozo[1], Rossana C. Jaca[1] and Luis A. Godoy[2]

1. *Universidad Nacional del Comahe, Facultad de Ingeniería, Departmento Ingeniería Civil, Neuquén, Buenos Aires 1400, Argentina; sube_09@outlook.com, veropedrozo@gmail.com, rossana.jaca@fain.uncoma.edu.ar*
2. *Instituto de Estudios Avanzados en Ingeniería y Tecnología (IDIT), CONICET-Universidad Nacional de Córdoba, 5000 Córdoba, Argentina, luis.godoy@unc.edu.ar*

ABSTRACT

The localized settlement of columns in large metal industrial buildings induces out-of-plane displacements of side walls of the same order as the settlement, which may affect service conditions in the building. For a structural configuration formed by frames, side-walls and wall-girts, this work reports results from testing a small-scale model together with computational modeling of the full-scale structure. Dimensional analysis was used to scale the geometry and properties from full-scale to small-scale, leading to an overall scale factor of 1:15. Differential settlements having a controlled amplitude were imposed at the central column, and displacements were monitored using mechanical devices. The computational model employed shell elements for side-walls and wall-girts. Good agreement was found between tests and computer modeling. The results at the full-scale level, indicate that, for settlements likely to occur in granular soils, the associated lateral displacements exceed those allowed by current US regulations. Stiffening the structure was investigated by use of stiffer girts, as well as by reducing their spacing. The influence of frame height was also investigated. The overall conclusion is that out-of-plane displacements of side-walls may easily exceed allowable values unless they are specifically considered at a design stage.

KEYWORDS

Buckling, Finite elements, Settlement, Industrial buildings, Small-scale modeling, Wall-girts

INTRODUCTION

The effects due to localized settlements of part of the foundation in metal industrial buildings are not taken into account at a design stage; however, they frequently occur during the service life of a building. Such problems may become important when the building is constructed on compressible soils, in which the load-bearing capacity depends on soil type and moisture contents. Metal industrial buildings designed to process and store agricultural products are often built in zones with natural or artificial irrigation, in which the soil may lose part of its load-carrying capacity. Further, soil moisture may increase due to seasonal rains or due to accidents in an adjacent channel or piping system.

Light-weight industrial structures have low redundancy in their load-transfer mechanisms, so that differential settlements may cause changes in the way equilibrium is provided by the frame and roof system. Of special concern in this paper are settlements between adjacent columns or at the corners of a building.

Damage due to vertical settlements may affect the main resisting structure, secondary elements, and equipment protected by the construction, and their consequences are typically observed as out-of-plane displacements in the side walls. Such lateral displacements arise due to buckling of the side walls under imposed vertical displacements [1]. All this may weaken the overall structural strength and stiffness of the building; and may also affect the service conditions of the building, including the normal functioning of large sliding doors.

Only a small number of references have focused on this problem with reference to sustainability issues [2]. Effects of support settlements have been considered in metal cylindrical shells [3]. Buckling of storage tanks due to support settlements was studied by Godoy and Sosa [4], Zhao et al. [5], Gong et al. [6], Cao and Zhao [7] and Fan et al. [8]. Darmawan [9] reported severe damage induced by column settlement on a metal frame structure. The non-linear behavior of soil in a two-story frame building was studied by Agrawal and Hora [10]. All those results were based on computational modeling. Codes of practice, such as ASCE [11], specify limits to lateral displacements of the side walls in metal buildings in the order of H/400 to H/600, where H is the height of the building. Such limits were established based on wind pressures acting on the building and do not considerer either buckling or settlement of supports.

Previous works by the authors showed that the out-of-plane displacements in side walls due to vertical settlements are larger than allowed values when considering the main resisting structure but neglecting the contributions of secondary elements in side walls [1]. This paper aims to evaluate the influence of wall-girts as a strengthening aid in cases of localized support settlement in metal industrial buildings.

FULL-SCALE PROTOTYPE AND REDUCED-SCALE PHYSICAL MODEL

A physical model was built and tested in this research in order to obtain empirical evidence to validate computer models. A full-scale prototype was first defined and then a small-scale model was built using similitude theory (see, for example, [12]).

Full-scale prototype

With reference to Figure 1, the geometry of the prototype was characterized by height H, height of columns h, frame width B, and span between frames ℓ. The main resisting structure is formed by a set of steel frames, whereas secondary elements include wall panels which are strengthened by wall-girts and roof purlins.

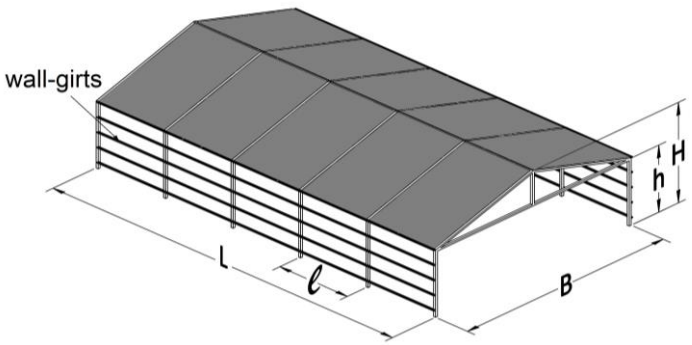

Fig. 1 – Geometry used to describe full-scale and small-scale model in this work.

Previous studies [1] showed that settlement of a single column may have severe consequences on the side walls that extend to the next frame in both directions, but do not extend further to other frames. For this reason, the fabricated model was limited to three frames, which includes the side walls with five wall-girts, whereas the computational model could use symmetry conditions and reduce the domain of interest to two frames, as shown in Figure 2.a. The initial case-study investigated had H = 6m, h = 4m, ℓ = 5m, and B = 15m. Separation between girts, shown in

Figure 2.a, was s = 0.90m. Such secondary elements are considered in this work to investigate their influence in reducing side displacements. The roof purlins and wall-girts were assumed as a C-shape cold-formed cross section with dimensions shown in Figure 2.b. The values of dimensions for the assumed prototype are given in the second column in Table 1.

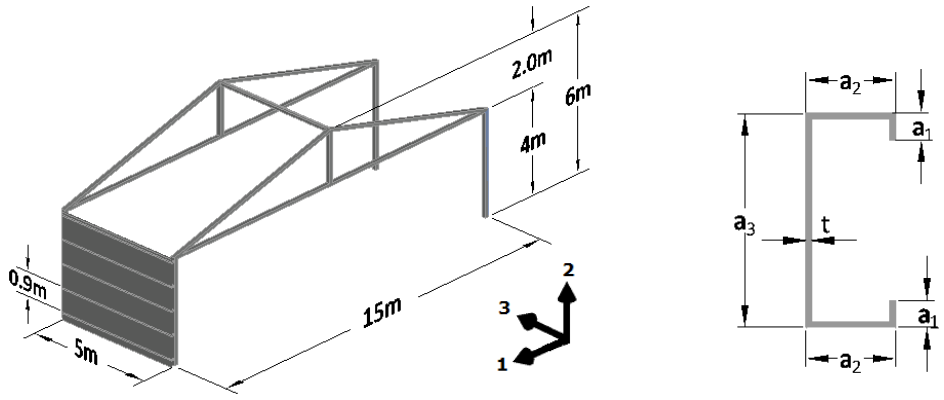

(a) *(b)*

Fig. 2 – Geometric characteristics, (a) Symmetric geometry investigated by computational analysis in this work for the prototype, (b) Cross-sectional geometry of C-shape cold-formed wall-girts.

Tab. 1: Geometry of cross section of wall-girts (Figure 2.a). Values in [mm].

	Prototype	Small-scale model of prototype	Small-scale simplified model
a_1 [mm]	15	1	0
a_2 [mm]	50	3	2
a_3 [mm]	120	8	6
t [mm]	3.2	0.07	0.22

The side-walls in the prototype were initially assumed with a trapezoidal T1010 section. However, for both computational and experimental modeling, the cross section was substituted by another one with uniform thickness, in which the thickness was evaluated to have the same modulus of inertia as the trapezoidal section. This yields an equivalent thickness of side walls equal to t_{wall}=9.6mm. The modulus of elasticity of steel was assumed as E_p = 204GPa, with density ρ_p = 7850Kg/m^3.

Reduced-scale physical model

The full-scale building was modeled down to reduced-scale dimensions, and the resulting small-scale model was fabricated and tested during this research. Geometric similitude was used to scale the geometry, together with a similitude to represent the constitutive materials. The overall dimensions in Figure 2.a were scaled down to B_m = 1m, so that there is a scale factor in the geometry given by:

$$\alpha_A = \frac{B}{B_m} = 15 \quad (1)$$

This scale factor α_A was used to identify the geometry of the small-scale physical model, leading to model dimensions H_m = 400mm, h_m = 267mm, ℓ_m = 333mm, and s_m = 60mm. However, because of the considerable differences between the overall building dimensions and the side wall panels and wall-girts, different scale factors were used to identify the thicknesses, thus leading to a geometrically distorted model.

The adopted material for the main frame in the model is aluminum with a square cross-section having 12mm sides, with elastic properties are E = 70GPa, μ = 0.33. The side walls were made of acetate sheets with commercially available thickness t_m = 0.22mm. Mechanical properties for acetate were evaluated following ASTM D882-02 [13] and the values were E_m = 2294MPa (Young ´s modulus) and μ_m = 0.4 (Poisson´s modulus), the density were also measured (ρ_m = 1320Kg/m^3). The material scales for acetate are thus given by:

$$\theta = \frac{E_p}{E_m} = 89 \quad and \quad \gamma = \frac{F_p}{F_m} = \frac{\rho_p * (\ell * h * t)}{\rho_m * (\ell_m * h_m * t_m)} \quad with \quad \frac{\rho_p}{\rho_m} = 5.95 \tag{2}$$

where γ is the ratio between the weight of side wall panels (F_p for prototype and F_m for small-scale model). The scale factor for thicknesses is

$$\alpha_B = \frac{t}{t_m} = 43.6 \tag{3}$$

As required, the relation between θ, γ, and α satisfies the condition

$$\theta = \frac{\gamma}{\alpha_A * \alpha_B} \tag{4}$$

The third column in Table 1 (small-scale model of prototype) shows the cross section of a wall-girt under a scale factor 15 and 43.6 for thickness. However, such details could not be achieved in the small-scale model, with the consequence that a simplified section with dimensions shown in the fourth column of Table 1, based on an equivalence of the moment of inertia, were used.

(a) *(b)*

Fig. 3 – Model testing at a 1:15 geometric scale: (a) General view of the three-frame configuration in the small-scale model; (b) Device used to impose vertical displacements at the central column.

The settlement was induced in the central column, as shown in Figure 3.b. The settlements of the column and the out-of-plane displacements were measured with 0.01mm precision. The relations between the imposed settlements in prototype and model are shown in Table 2. Limits in prototype settlement are usually given as 25mm in civil engineering structures (see, for example, [14] [15]).

Tab. 2: Applied settlements in prototype and model.

Settlement [mm]	Prototype	5	7	9	10	20	25
	Model	0.33	0.47	0.6	0.67	1.33	1.67

EXPERIMENTAL RESULTS FOR THE SMALL-SCALE PHYSICAL MODEL

Testing was carried out by imposing a vertical displacement at the central column, thus causing a relative displacement δ with respect to the side frames. To facilitate visualization of points on the side walls, a grid formed by 30 × 30 mm squares was drawn in the model. As a consequence of this vertical displacement, there are out-of-plane displacements w on the side walls, forming diagonal shear bands with alternate inwards and outwards displacements. These bands form a V-shape with a vertex at the joint between wall-girts and column, being symmetric with respect to the central column in which δ is imposed. The displacements in the model are scaled up to the prototype dimensions by use of the scale factor α_A = 15, so that inwards and outwards displacements in the horizontal direction of the prototype can be plotted in Figure 4.

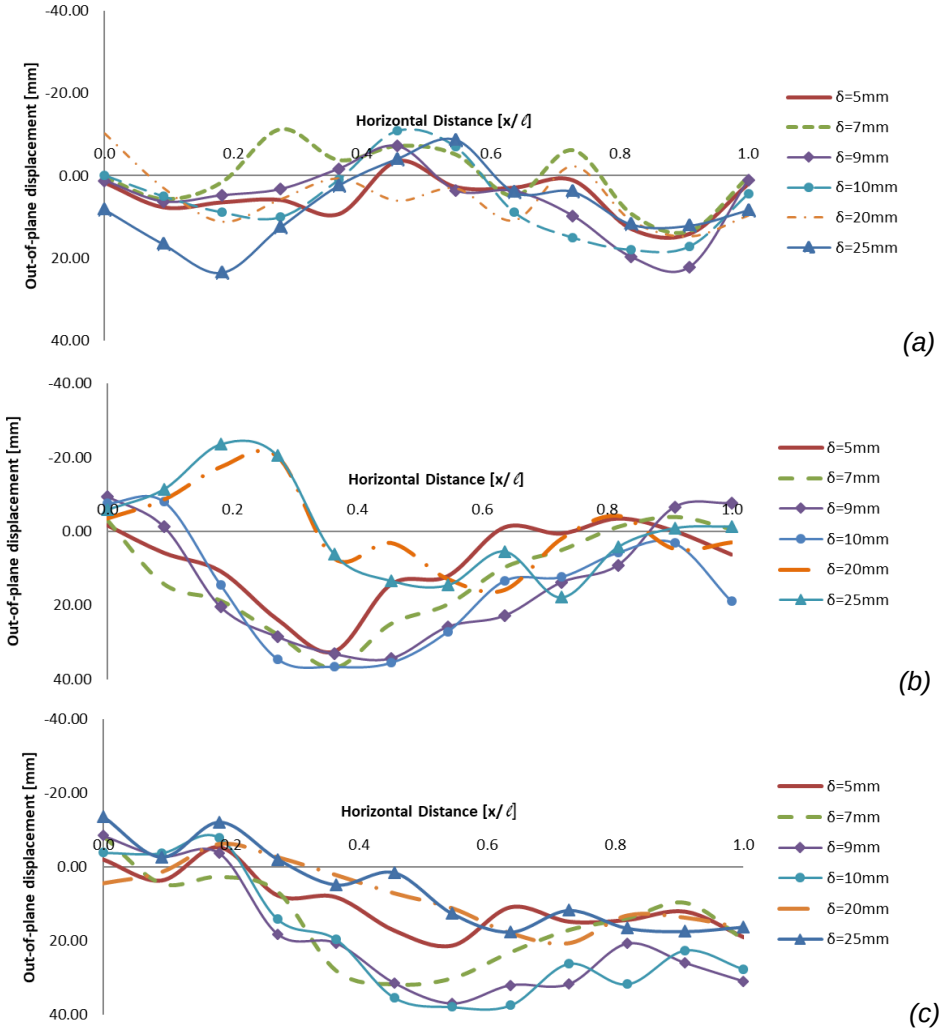

Fig. 4 – Out-of-plane displacements (w) due to vertical settlement 5mm < δ < 25mm. The horizontal axis spans from 0 at the central column to x/ℓ = 1 at the next column. (a) Variation at 0.90m (z/h=0.225) from bottom level; (b) at 2.25m (z/h=0.563) from bottom level; (c) at 3.15m (z/h=0.79) from bottom level.

The deflected shape is a function of settlement, with nonlinear changes in shape and amplitude. For example, for δ = 5mm there are outward displacements in Figure 4.b with a maximum of about w = 35mm; this increases to close to w = 50mm at δ = 10mm; but for larger settlements δ = 20mm and δ = 25mm the lateral displacement becomes inwards in the order of w = 25mm. On the other hand, the number of bands increases with increasing δ. A reduction in w is seen to occur near the columns and wall-girts, which induce a restraint to lateral deflections. This effect can also be

noticed in Figure 5, in which the vertical variation of displacements along the central column and at two intermediate positions, is shown, together with the location of the wall-girts in elevation.

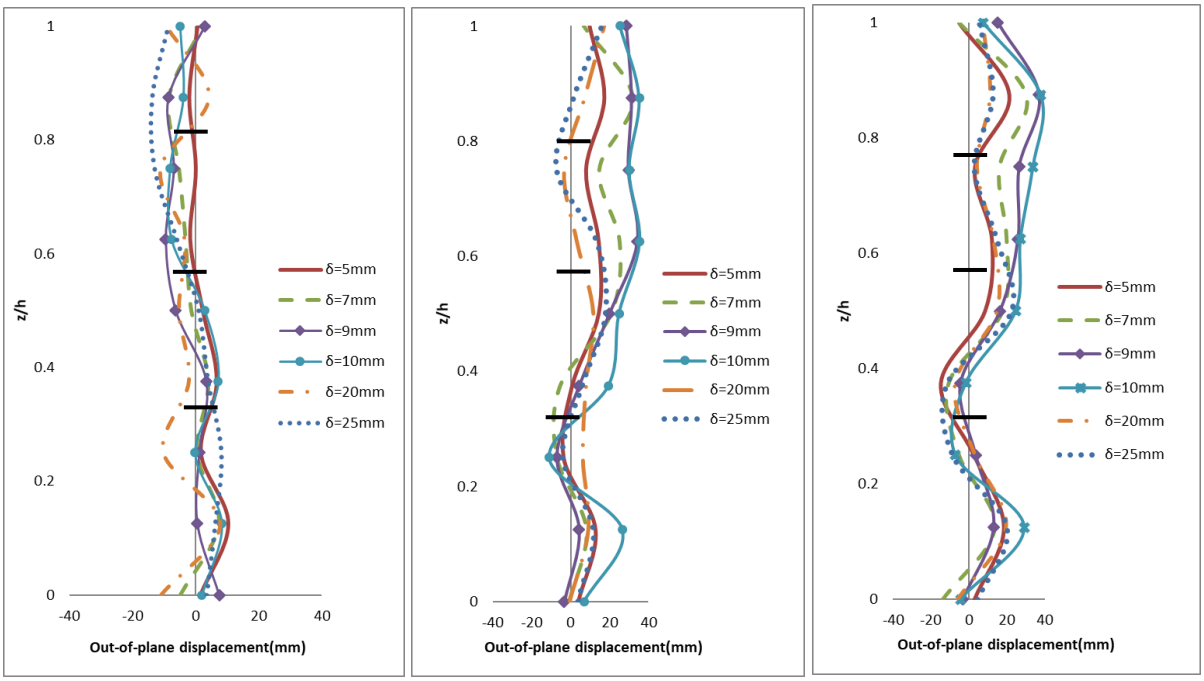

(a) (b) (c)

Fig. 5 – Out-of-plane displacements (w) due to vertical settlement 5mm < δ < 25mm. (a) Variation at the central column(x/l=0); (b) at 2.27m(x/l=0.45) from central column; (c) at 2.72 (x/l=0.54) from central column.

A summary of results is shown in Table 3, in which inward displacements (w) are identified with negative values; and outward displacements are positive values. The largest outward displacement occurs for δ = 10mm, whereas the largest inward displacement occurs for a low value δ = 5mm.

Tab. 3: Maximum and minimum lateral displacements, in [mm].

δ [mm]	5	7	9	10	20	25
Maximum [outward]	32.4	36.9	36.9	37.8	27.3	33.3
Minimum [inward]	-30.2	-29.1	-30.0	-29.3	-24.8	-25.7

Displacement maps are plotted in Figure 6. Wall-girts are also shown in the figures to facilitate visualization of restrains introduced by secondary elements. The general trend is the development of inclined bands, with an angle close to 45° for δ = 10mm, and the inclination reduces to about 32° for δ = 25mm. There is a clear incidence of wall-girts on displacements, not just by affecting their amplitude but also by modification of the shear bands. Previous computational models [1] showed continuous bands because wall-girts were not included in the model.

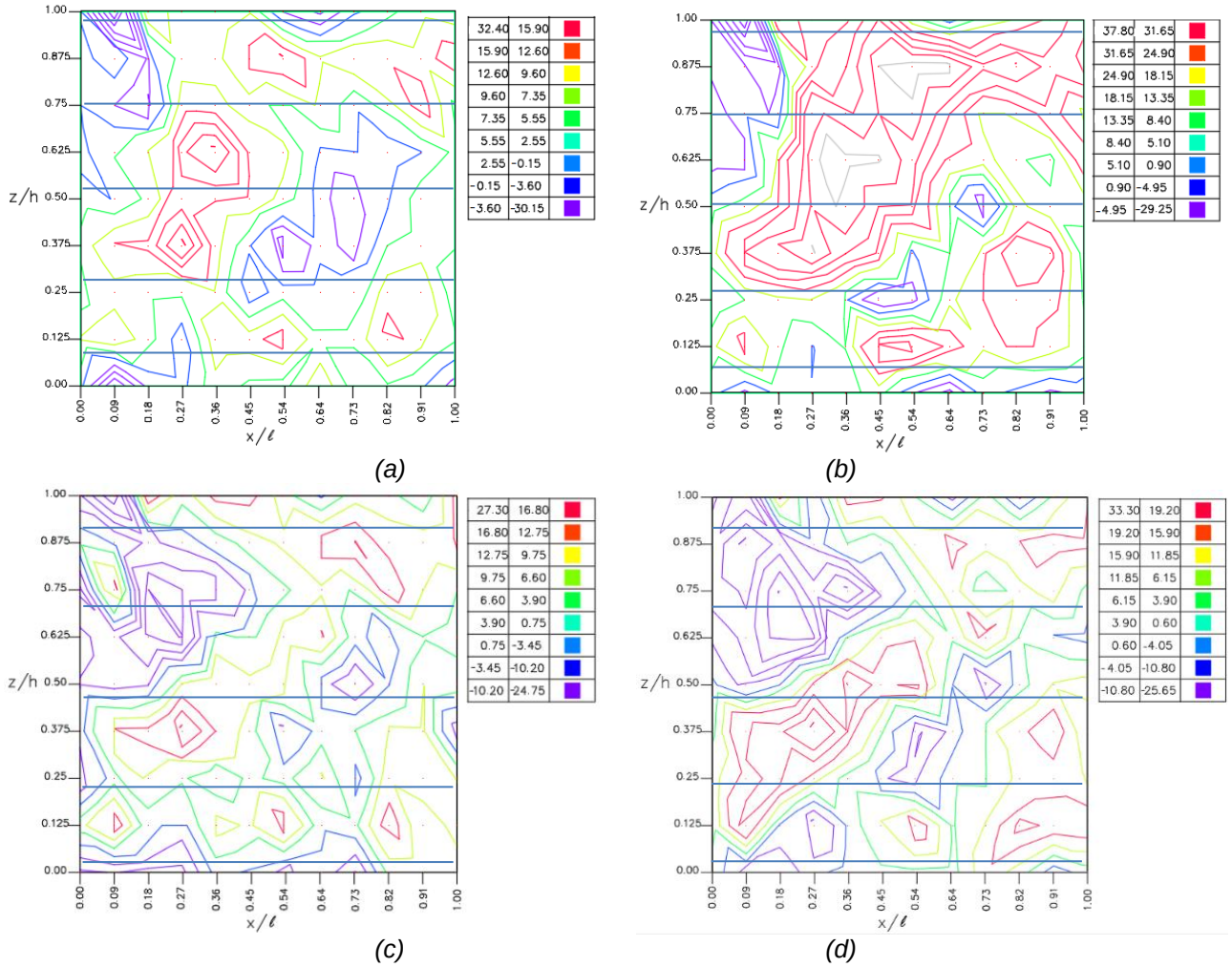

Fig. 6 – Maps of out-of-plane displacements for settlements (a) δ = 5mm; (b) δ = 10mm; (c) δ = 20mm; (d) δ = 25mm

FINITE ELEMENT MODEL AT FULL-SCALE

Configuration investigated

The prototype structure has been investigated using a finite element model [16]. The analysis requires modelling of the frame, wall-girts and side-walls, as shown in Figure 2.a. Structural symmetry was used to reduce the number of unknowns in the model. Rectangular shell elements (identified as S4R5 in ABAQUS) with five DOF per node and four nodes per element were employed. A finite element mesh with 32,000 elements was defined by means of convergence studies and has been used in the computations reported in the following sections. Wall-girts were modelled using shell elements and the assumed dimensions (120mm×50mm×15mm cross-section and 3.2mm thickness) are shown in Figure 2.b. The separation between girts was 0.90m, thus including five wall-girts in elevation.

Some details regarding modeling of joints need to be presented. (a) Girts are connected with columns by means of welds, which are represented in the model by joint elements identified as “Tie” elements. (b) Side panels are connected with girts by means of screws, and these are modeled by “Beam” joint elements, which restrain displacements and rotations. A total of 100 screws were used in the model, of which 20 were applied in each girt at a spacing of 260mm.

With reference to Figure 2.a, boundary conditions U1 = U2 = U3 = UR1 = UR3 = 0 are imposed at the base of columns that do not have settlement; conditions U1 = UR1 = UR3 = 0, and U2 = 25mm are imposed at the base of the column with settlement; condition U3 = UR1 = UR2 = 0 are used to represent symmetry on the central column; condition U1 = U2 = U3 = 0 is imposed at the joint between wall-girts and column; and conditions U1 = U2 = U3 = UR1 = UR2 = UR3 = 0 are imposed at the screw joints.

Computational results for the full-scale prototype

A geometrically non-linear static analysis was carried out to investigate the full-scale prototype shown in Figure 2.a. The assumed modulus of elasticity was E = 204GPa, with Poisson ratio μ = 0.3. The imposed vertical settlement was taken as δ = 5mm, 10mm, 20mm, and 25mm, to replicate the experiments. The dimensions of girts were considered as in Figure 2.b. To reduce computations, symmetry was used so that only the right-hand side panel is represented in the finite element discretization, as shown in Figure 2.a, and settlement is imposed on the column to the left of this figure.

Results for the case δ = 25mm are shown in Figure 7.a, leading to maximum out-of-plane displacements w = 25.7mm (inwards) and 33.3mm (outwards). The bands are seen to cross the lines of girts in this case, thus forming continuous diagonals. The values are compared with those measured in the tests (see Figure 6.d) and there are only 5% differences in maximum values, with some differences in the diagonal patterns. In the finite element model the displacements w affect the complete side-wall whereas they tend to be localized in the region where the settlement is imposed in the tests. The same number of shear bands occurs in both computational and physical models, with similar inclination.

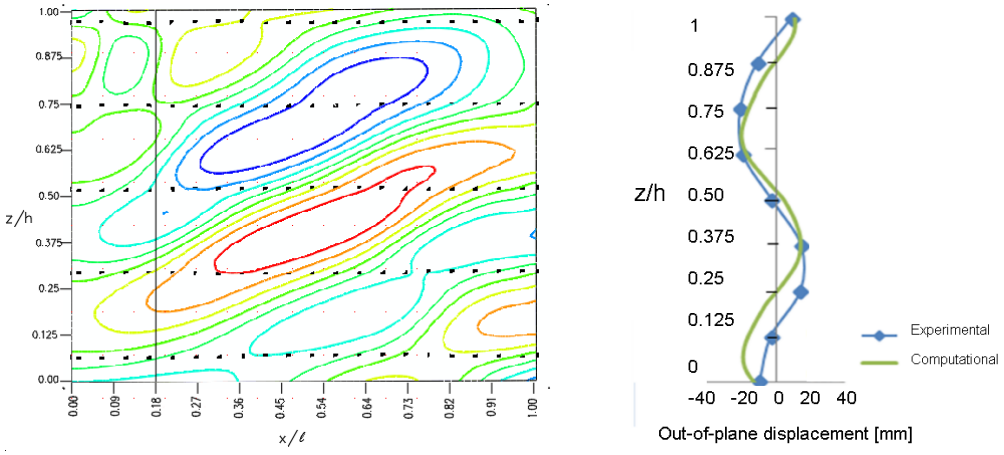

(a) *(b)*

Fig. 7 – Computational results for δ = 25mm. (a) Map of out-of-plane displacements; (b) Out-of-plane displacements plotted in elevation z/h, at a distance x/l= 0.18 measured from the central column, and comparison with experiments.

A comparison of vertical variation of displacements is shown in Figure 7.b. The computational results seem to capture the main features of the behavior as detected in the physical model, and this provides confidence in pursuing a more thorough understanding of behavior based on computational modeling.

INFLUENCE OF PARAMETERS CONTROLLING THE RESPONSE

To understand the significance of the lateral displacements reported in the previous section, it is important to refer to what is acceptable in practice. ASCE [11] rules establish limits to out-of-plane deflections which range between H/400 and H/600; in the present case this means bounds between 15mm and 10mm. Such bounds are clearly exceeded by the values reported in the present

study. Thus, it would be desirable to understand what parameters may affect the response in order to reduce such lateral displacements.

Influence of strengthening the cross section of wall-girts

Computational modeling is used in this section to illustrate the influence of the stiffness of wall-girts on lateral deflections under a given settlement. In each case the separation between girts remains fixed at 0.90m, and the cross sections are modified as shown in Table 4. The thickness of the wall-girts is taken as t = 3.2mm, and the overall dimensions change from cases P1 to P7. The case already taken as case study in the previous section is P1. Although typical cross sections in practice range from P1 to P5, two stiffer cases, P6 and P7, were also investigated to understand what would it take to improve the behavior.

Tab. 4: Geometry of cross section of wall-girts considered in the analyses. Variables a_1, a_2, a_3, t, are illustrated in Figure 2.b. Values in [mm].

	a_1	a_2	a_3	t
P1	15	50	120	3.2
P2	20	50	140	3.2
P3	20	60	160	3.2
P4	25	70	180	3.2
P5	25	70	200	3.2
P6	25	80	220	3.2
P7	20	80	240	3.2

Results are shown in Figure 8. The order of these figures corresponds to the order of girts in Table 4. In all cases considered in this section, a settlement δ = 25mm is imposed, and separation between girts is 0.90m. As expected, lateral displacements decrease with increasing stiffness of girts. For “weak” girts, the shear bands are continuous and affect the complete panel across girts. For “robust” girts the shear bands are interrupted and extreme values of w occur between girts.

In comparison with girt P1, the sections P2 and P3 cause a reduction of 19%, but more significant changes are found for P4 (30%) and P7 (52%) always measured with respect to P1. The w values for P7 are 22.2mm (outwards) and -21.4mm (inwards), which are about half of those computed for P1. A summary of results is shown in Table 5. Notice that acceptable values according to ASCE (H/400 or H/600) are not met in any case shown in Table 5.

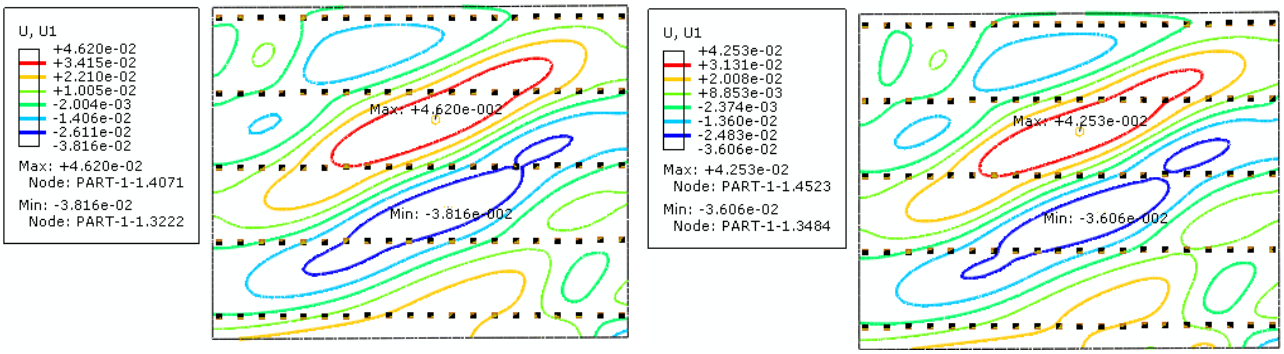

(a) *(b)*

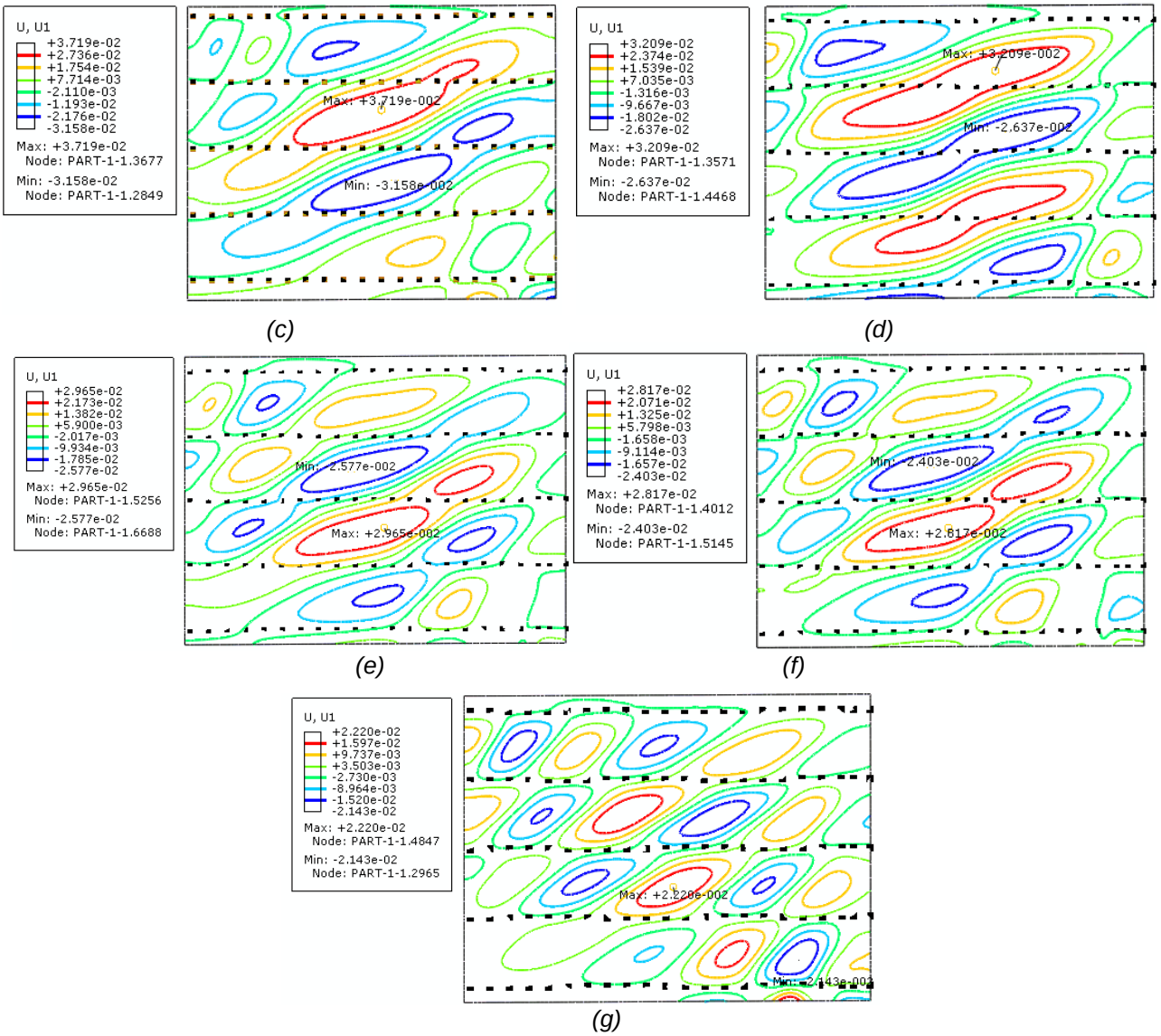

Fig. 8 – Out-of-plane displacements for various cross-sections of girts for δ = 25mm and s = 0.90m. (a) P1, (b) P2, (c) P3, (d) P4, (e) P5, (f) P6, (g) P7.

Tab. 5: Extreme out-of-plane displacements (outwards and inwards) for wall-girt sections of Table 4. Data: H = 6m; s = 0.9m; δ = 25mm.

Wall-girt cross-section	Displacement [mm]		Difference with respect to P1
P1	46.2	-38.1	
P2	42.5	-36.0	-8%
P3	37.2	-31.6	-19%
P4	32.1	-26.3	-30%
P5	29.6	-25.7	-36%
P6	28.2	-24.0	-39%
P7	22.2	-21.4	-52%

Influence of separation between wall-girts

To understand the influence of the separation between wall-girts, their values were reduced from 0.90m to 0.70m and 0.60m, as shown in Table 6. Changes are calculated by comparing the displacements for P1, P2, P3, P4, P5, P6, and P7 in this table with displacements for P1 in Table 5. Because there are positive and negative extreme values, the largest value is considered to compute changes.

Tab. 6: Influence of separation between wall-girts on lateral displacements, for settlement δ = 25mm. Ridge height H = 6m.

Wall-girt cross-section	Number of wall-girt	Separation [m]	Displacement [mm]		Difference with respect to P1 in Table 3
P1	7	0.6	43.7	-35.2	-6%
P2	7	0.6	37.8	-22.4	-40%
P3	7	0.6	32.1	-23	-39%
P4	7	0.6	25.3	-19.4	-48%
P5	7	0.6	20.7	-16.1	-57%
P6	7	0.6	16.6	-13.8	-63%
P7	7	0.6	14.3	-12.7	-68%

For reasons of brevity, maps of lateral displacements are not shown here, but the number of bands increases for separation 0.60m, with an inclination of approximately 30°. There is an interruption of bands for P7 caused by the stiff girts. The practical case P5 with separation 0.60m shows a 57% reduction with respect to the reference case P1, but values still exceed those allowed by ASCE specifications.

Influence of ridge height

The influence of the ridge height H of the frame on the deflected pattern was next investigated under an imposed settlement δ = 25mm.

First, consider H = 10m. A summary of results is shown in Table 7 for girt separations in the range s = 0.90m to s = 0.50m, and for various cross-sections of girts. Changes in the last column were computed with respect to values for P1 in the first row.

Tab. 7: Out-of-plane displacements for a frame with H = 10m under an imposed settlement δ = 25mm

Wall-girt cross-section	Separation (m)	Displacement [mm]		Difference with respect to P1
P1	0.9	43.84	-44.8	
P2	0.9	41.92	-35.9	-20%
P3	0.9	34.9	-31.1	-31%
P4	0.9	26.9	-25.3	-44%
P5	0.9	24.5	-27.1	-44%
P6	0.9	25.4	-22.2	-50%
P7	0.9	24.2	-23.4	-48%

P1	0.5	36.4	-30.5	-32%
P2	0.5	28.6	-24.5	-45%
P3	0.5	23.5	-20.6	-54%
P4	0.5	15.9	-15.2	-66%
P5	0.5	14.2	-11.9	-73%
P6	0.6	13.66	-13.7	-69%
P7	0.6	11.4	-13	-74%

Tab. 8: Out-of-plane displacements for a frame with H = 8m under an imposed settlement δ = 25mm.

Wall-girt cross-section	Separation (m)	Displacement [mm]		Difference with respect to P1
P1	0.7	37.12	-38.21	
P2	0.7	32.06	-32.58	-15%
P3	0.7	31.90	-27.03	-29%
P4	0.7	26.62	-24.66	-35%
P5	0.7	19.9	-16.3	-57%
P6	0.7	17.2	-15.9	-58%
P7	0.7	17.04	-14.79	-61%

Because of the increase H with respect to the previous results reported in this work for H = 6m, the allowable lateral displacements increase to H/400 = 25mm and H/600 = 17mm. For a spacing s = 0.90m, acceptable lateral displacements are reached for girts P4 to P7. Separations of s= 0.50m and s = 0.60m could be acceptable for all alternatives considered, except for P1.

Second, ridge height H = 8m was consider as an intermediate case, and results are shown in Table 8. The limit value for lateral displacements in this case is H/400 = 20mm; thus, wall-girts identified as P5, P6 and P7 with s = 0.70m yield satisfactory side displacements.

Wall-girt size and separation for buildings of different ridge height

Based on results of the finite element analyses, the range of wall-girt size and separation which lead to acceptable displacements in industrial buildings is shown in Figure 9. For ridge height equal to or larger than 6m, the displacements remain within acceptable values for wall-girts equal to or larger than P5 (200mm), with separations smaller than 0.6 m. For buildings with H ≥ 8m, displacements remain acceptable provided wall-girt size is at least P4 (180 mm) and separation is s ≤ 0.6m. Finally, admissible displacements in buildings with H ≥ 10m are achieved by using P4 or larger, with s ≤ 0.9m, or else P2 (140mm) with s ≤ 0.5m.

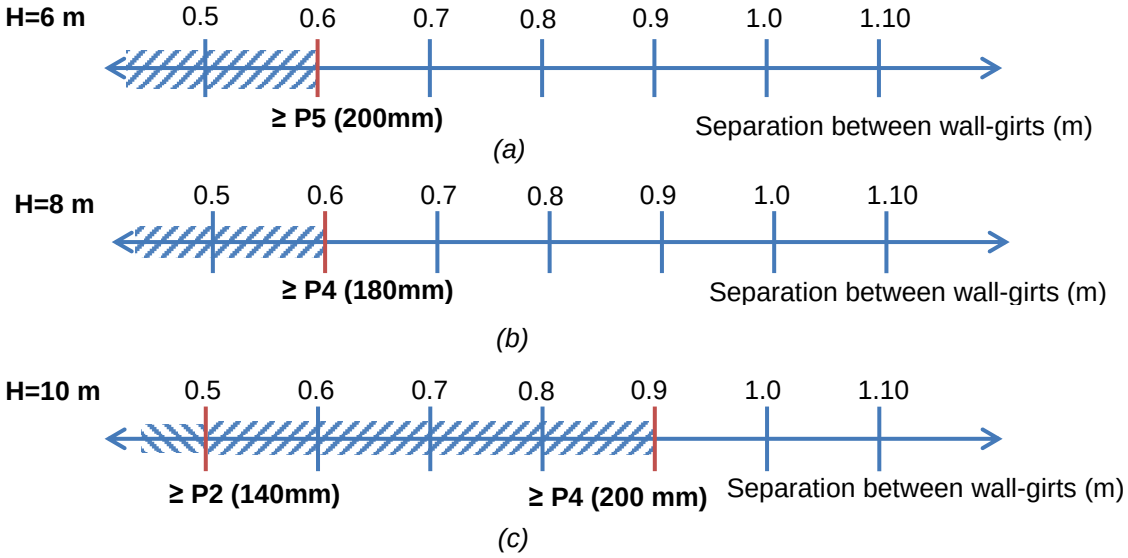

Fig. 9 – Wall-girt configuration for industrial buildings having different ridge height H. (a) H = 6m; (b) H = 8m; (c) H = 10m. Shaded separations are acceptable.

COMPARISON WITH OUT-OF-PLANE DISPLACEMENTS UNDER WIND LOADS

Wind loaded industrial buildings are investigated in this section in order to compare out-of-plane displacements with those derived from foundation settlements. For low rise buildings, i.e. H≤20m, ASCE [11] specifies the following expression for the pressure q_z on the windward walls:

$$q_z = 0.613 K_z K_{zt} K_d V^2 \quad (5)$$

where V is the wind speed in [m/s], and q_z is evaluated in [N/m^2] at elevation z. K_{zt} is the topographic factor (with unit value for flat terrain); K_d refers to the direction of wind and a value K_d= 0.85 was adopted in this case; and K_z is the exposure factor, and K_h=0.9 was adopted in this case. Wind speed V=48m/s was assumed as a reference value for the design of the industrial building. For a partially enclosed building and for the internal spans between columns, the internal pressure coefficient is (GCpi) =±0.55 whereas the external pressure coefficient is (GCpe) = 0.45.

The maximum displacements computed for the side walls for different locations in elevation are listed in Table 9, together with the limit displacements U_{limit} evaluated as H/400 according to ASCE provisions [11]. To perform calculations, the assumed stiffening was the weakest configuration investigated, i.e. P1 with separation s=0.90m.

Tab. 9: Comparison of out-of-plane displacements for wind and for support settlement, in [mm].

		H=6m	H=8m	H=10m
U_{limit}		15	20	25
U_{max} due to V=48m/s		**1.70**	**1.13**	**1.73**
U_{max} due to support settlement	δ = 3mm		1.58	1.05
	δ = 5mm	1.34	3.70	1.84
	δ = 7mm	1.48		2.89
	δ = 10mm	13.54	20.5	17.6
	δ = 15mm			23.06
	δ = 25mm	46.0	45.2	44.8

The resulting out of plane displacements for wind speed V=48m/s are lower than those specified by the design provisions, and are one order of magnitude lower than those obtained for a support settlement equal to δ = 25mm.

To identify the level of settlements that induce out-of-plane displacements of similar value to those due to wind, results for several values of δ are listed in Table 9. The out-of-plane displacements due to wind are similar to those computed for rather small settlements: δ = 7mm for H=6m, δ = 3mm for H=8m, δ = 5mm for H=10m.

Values of U_{limit} are also shown in Table 9, with the consequence that settlements up to δ = 10mm are acceptable in terms of design provisions. Notice that equivalent values under wind would require wind speed much higher than that adopted for the design of the building.

The first conclusion of this comparison is that the out-of-plane dispacements under a support settlement is dominant with respect to wind effects. A second conclusion is that whenever settlements of supports can occur, then some measures should be adopted to control their effects (i.e., following Item 1.3.3 Self-Straining Forces in Ref. [11]) because wind design does not cover this aspect of behavior of lateral walls in desing buildings. Possible remedial actions depend on their economic evaluation in each case, but may include strengthening the side walls by wall-girts, as described in this work; limiting the settlements by strengthening the soil or the foundation; and/or reducing the presence of water around the building.

CONCLUSIONS

Lateral displacements of side walls induced by a vertical settlement of a column were investigated in this work for metal industrial buildings. Two approaches were used in the research, one based on a physical small-scale model and another one based on a geometrically non-linear finite element model of the structure. The computational modeling was validated by comparison with the small-scale model tested. Finite element results included maps of lateral displacements for various wall-girt configurations for a given settlement at a column.

Based on the results, some conclusions may be drawn:

- The computational model discussed in this work adequately represents displacement levels obtained in the physical model. The maximum displacements tend to be located at the center between wall-girts.
- Because side-walls made with acetate are very flexible in the physical model, the deflected patterns tend to be interrupted at wall-girts, and there are some differences with patterns obtained in the finite element model, which tend to be continuous bands.
- Lateral displacements obtained in this work are considerably reduced (by approximately 50%) with respect to previous studies, in which the influence of wall-girts was not considered [1].
- Decreasing the separation between wall-girts and increasing their cross-section cause significant reductions in lateral displacements, and also change the deflected pattern by an interruption in shear bands as they cross the wall-girts.
- To satisfy limits to displacements established by current ASCE regulations, the wall-girt configurations are more stringent in shorter than in taller frames, as given by ridge height. Such limits in ASCE were established based on wind effects and do not take into account effects due to settlement or buckling.
- The out of plane displacements in side walls computed for small settlements (in the order of 5mm) are similar to those due to wind speed as used at the design stage.
- Special attention should be given to vertical support settlements larger than 10mm and they should be monitored during the service life of the structure. Remedial actions may include stiffening the lateral walls by means of wall-girts or improving the soil/foundation capacity.

ACKNOWLEDGEMENTS

This research was supported by a grant from Universidad Nacional del Comahue (PI Rossana C. Jaca), and by a PUE grant awarded by CONICET to IDIT (Instituto de Estudios Avanzados en Ingenieria y Tecnologia) (PI Luis A. Godoy and Sergio A. Elaskar).

REFERENCES

[1] Fernández, S., Jaca, R.C., Godoy, L.A., 2015. Behavior of wall panels in industrial buildings caused by differential settlements. Structural Engineering and Mechanics, vol. 56 (3): 1-18, dx.doi.org/10.12989/sem.2015.56.3.443.

[2] Švajlenka, J., Kozlovská, M., Pošiváková, T., 2018. Analysis of selected building constructions used in industrial construction in terms of sustainability benefits. Sustainability, vol. 10: 4394, doi:10.3390/su10124394.

[3] Jonaidi, M., Ansourian, P., 1998. Harmonic settlement effects on uniform and tapered tank shells. Thin-Walled Structures, vol. 31: 237-255, doi.org/10.1016/S0263-8231(98)00007-X.

[4] Godoy, L.A., Sosa, E.M., 2003). Localized support settlements of thin-walled storage tanks. Thin-Walled Structures, vol. 41: 941-955, doi.org/10.1016/S0263-8231(03)00043-0.

[5] Zhao, Y., Cao, Q.S., Xie, X.Y., 2006. Floating roof steel tanks under harmonic settlement: FE parametric study and design criterion. Journal of Zhejiang University, Science A, vol. 7(3): 398-406, doi.org/10.1631/jzus.2006.A0398.

[6] Gong, J., Cui, W., Zeng, S., 2012. Buckling analysis of large-scale oil tanks with a conical roof subjected to harmonic settlement. Thin-Walled Structures, vol. 52(7): 143-148, doi.org/10.1016/j.tws.2011.12.011.

[7] Cao, Q.S., Zhao Y., 2010. Buckling strength of cylindrical steel tanks under harmonic settlement. Thin-Walled Structures, vol. 48(6): 391-400, doi.org/10.1016/j.tws.2010.01.011.

[8] Fan, H., Chen, Z., Shen, J., Cheng, J., Chen, D., Jiao, P., 2016. Buckling of steel tanks under measured settlement based on Poisson curve prediction model. Thin-Walled Structures, vol. 106: 284-293, doi.org/10.1016/j.tws.2016.05.009.

[9] Darmawan, M.S., 2009. A case-study of structural assessment of steel structure subjected to differential settlement of foundation. 1st Int. Conf. on Rehabilitation and Maintenance in Civil Engineering (Solo, Indonesia), 312-320.

[10] Agrawal, R., Hora, M.S., 2010. Effect of differential settlements on nonlinear interaction behavior of plane frame-soil system. ARPN Journal of Engineering and Applied Sciences, vol. 5(7): 75-87.

[11] ASCE STANDARD ASCE/SEI 7–10, 2010, Minimum Design Loads for Buildings and Other Structures, American Society of Civil Engineers, Reston, VA, USA.

[12] Szirtes, T., 1998. Applied Dimensional Analysis and Modeling (McGraw Hill) 853 pp.

[13] ASTM D882–02, 2002. Standard Test Method for Tensile Properties of Thin Plastic Sheeting. American Section of the International Association for Testing Materials, USA.

[14] USACE EM 1110-1-1904, 1990. Settlement analysis (U.S. Army Corps of Engineers) 205 pp.

[15] Bowles, J.E., 1988. Foundation Analysis and Design. 4th Edition (Ed. McGraw Hill Singapore) 1230pp.

[16] ABAQUS, 2010. Abaqus Inc., Dassault Systèmes, Rhode Island, USA.